Deltares

Vlaamse Baaien Flexible Mesh Model (VlaBa-FM)

Vlaamse Baaien Flexible Mesh Model (VlaBa-FM)

Author(s)
Marlies van der Lugt
Jebbe van der Werf
Björn Röbke

Vlaamse Baaien Flexible Mesh Model (VlaBa-FM)

Client	Vlaamse KustVisie
Contact persons	Marlies van der Lugt
Reference	
Keywords	Vlaamse Baaien, Zeebrugge, Vlaamse KustVisie, Delft3D-FM, Delft3D-4, Morphodynamic modeling, Hydrodynamic modeling

Documentdetails

Version	0.2
Date	04-03-2020
Project number	1210301-001
Document ID	1210301-001-ZKS-0009
Pages	33
Status	final

Authors

Marlies van der Lugt		
Jebbe van der Werf		
Björn Röbke		

Doc. Version	Authors	Review	Approve	Publish
0.1	Marlies van der Lugt	Mick van der Wegen	Toon Segeren	
	Jebbe van der Werf			
	Björn Röbke			

Samenvatting

Binnen het *Vlaamse Kustvisie* project ontwikkelt de Vlaamse Overheid een langetermijn strategie (tot 2100) voor kustbescherming. Numerieke modellen vormen gereedschap om de hydro-morfodynamische effecten van mogelijke verdedigingsstrategieën op de Vlaamse kust te beoordelen. Deltares lanceerde onlangs de Delft3D-FM (Flexible Mesh) software (zie bijvoorbeeld Martyr-Koller et al., 2017) met 2D morfologie. Met deze software kunnen snellere simulaties worden gedraaid op een flexibel rooster dat fijnmazig is waar nodig en grof waar het kan. Dit rapport bespreekt de omzetting van het Delft3D VlaBa model van Röbke et al. (2018) naar Delft3D-FM en een vergelijking van de hydro-morfodynamische resultaten en rekentijden.

De vergelijking van hydro- en morfodynamica tussen de Delft3D-4 en Delft3D-FM modellen van het VlaBa model laat een consistent beeld zien en geeft daarmee vertrouwen in de morfodynamische resultaten van het nieuwe Delft3D-FM model. Vergelijking van waterstanden, stroomsnelheden en golfhoogte laat zien dat er minimale verschillen bestaan in tussen de hydrodynamische modelresultaten, maar toetsing aan observaties toont aan dat de voorspellende waarde van Delft3D-FM even goed is als Delft3D-4.
De rekentijd met Delft3D-FM is afgenomen met een factor 2 ten opzichte van zijn voorganger. We verwachten dat met aanstaande verbeteringen aan het parallelliseren van de berekening, de rekentijd nog verder zal afnemen.

Dit rapport laat zien dat de 2DH morfodynamische functionaliteit van Delft3D-4, zoals morfologische versnelling, meerdere sedimentfracties en baggeren en storten goed werken in Delft3D-FM voor middellange termijn morfodynamische modellen die een gebied ter grootte van 30x30 k m beschrijven. We adviseren om voor toekomstige studies van het Vlaamse Baaien gebied te werken met een *fit-for-purpose* ongestructureerd rooster om optimaal gebruik te kunnen maken van de roosterverfijningsmogelijkheden van Delft3D-FM.

Summary

Within the *Vlaamse Kustvisie* project, the Flemish Government is developing a long-term (until 2100) coastal protection strategy. Numerical models are part of the toolbox used to assess the hydro-morphodynamic impact of potential protection strategies on the development of the Flemish coast. Recently, Deltares launched the Delft3D-FM (Flexible Mesh) software (see e.g. Martyr-Koller et al., 2017) with 2D morphology. It enables faster simulations with a flexible mesh, a high resolution where required and a low resolution where allowed.This report describes the conversion of the Delft3D VlaBa model of Röbke et al. (2018) to a Deflt3D-FM version and a comparison in terms of hydro-morphodynamic results and computational times.

The comparison of hydrodynamics and morphodynamics as computed by Delft3D-4 and Delft3D-FM model shows a consistency and gives confidence in the capabilities of morphodynamic modelling with Delft3D-FM. Comparison to water levels, flow velocities and wave height shows that Delft3D-FM performs equally well as Delft3D-4

With Delft3D-FM the computation time is reduced by a factor 2. Further developments in partitioning of the computation are anticipated to improve the computation time.

For mid-term morphological models over a 30-km long domain, this report demonstrates that the 2DH morphodynamic functionality of Delft3D-4 such as morphological acceleration, multiple sediment fractions, dredging and dumping work well in Delft3D-FM. Therefore, this study gives confidence in developing the next generation morphodynamic models in the new model suite. In future studies of the Vlaamse Baaien region with Delft3D-FM it is advised to move to a fit-for-purpose unstructured grid tomake optimal use of the local grid refinement capabilities of Delft3D-FM.

Content

1 Introduction

1.1 Background

Within the *Vlaamse Kustvisie* project, the Flemish Government is developing a long-term (until 2100) coastal protection strategy. The coastal protection is aimed to evolve with the rising sea level. The measures will be developed considering the coastal functions of safety against flooding, ecology, economy (in particular navigation), and (other) social benefits. The measures considered include strengthening the current sea defense, shifting the sea defense seaward and building a new offshore dune belt with water in between the new and old sea defense. (http://www.kustvisie.be)

Numerical models are valuable tools to explore the hydro-morphodynamic impact of these proposed measures along the Flemish coast. Numerical modelling of Flemish coastal zone and the adjacent mouth of the Scheldt estuary is challenging for a number of reasons:

1 Complex physics: both tide, wind and wave forcing is important, graded sediment effects (especially the area near Zeebrugge with large amounts of fine sediments), density effects related to Scheldt fresh water discharge.
2 Large spatial (~100 km) and temporal scales (~10 years) of the area of interest, which leads to large computational demand.
3 Required high spatial model grid resolution (~10 m in the surf zone) and the associated small time step to ensure model stability, resulting in computationally-demanding simulations.

These numerical challenges have been tackled by multiple fit-for-purpose model schematizations (see e.g. De Maerschalck et al., 2017), including domain-decomposition (DD) Delft3D-4 models with potential internal boundary issues and impractical pre- and postprocessing, which required long computation times. One of the models that were used is the Delft3D VlaBa (*Vlaamse Baaien*) model of the mouth of the Scheldt estuary, focusing on the coastal area between Zeebrugge and The Netherlands and able to predict ~10 years of morphological change (Röbke et al., 2018).

Recently, Deltares launched the Delft3D-FM (Flexible Mesh) software (see e.g. Martyr-Koller et al., 2017) that overcomes the above-described model issues. It enables faster simulations with a new numerical scheme suitable to facilitate a flexible mesh, i.e. a high resolution where required and a low resolution where allowed, without the need of DD boundaries. Within Deltares Delft3D-FM is a focus area of software development, e.g. blending elements of the XBeach and Delft3D software enabling a seamless simulation of storms and normal-day conditions.

1.2 Objective

The general objective is to develop a Delft3D-FM morphological model of the Scheldt estuary and Belgian coastal zone to assess large-scale interventions in the Scheldt mouth. This report describes the first step, addressing the following research question:

How does the VlaBa-FM model for 10 years of morphodynamics of the Scheldt mouth, converted from Delft3D-4, compare to the original VlaBa model in terms of hydro-morphodynamics and computational times?

1.3 Methodology

We followed the following steps :

1 Conversions of the Delft3D-4 VlaBa model to a Delft3D-FM model in a semi-automated way.
2 Comparison of Delft3D-FM computed water levels and flow velocities to Delft3D-4 and measurements for the year 2014.

3 Comparison of the Delft3D-FM and Delft3D-4 computed 10-year morphological development and dredging volumes, including variation of the morphological acceleration factor (MorFac), computational time step, and other model settings.
4 Exploration of computational speed-up by parallelization
5 Investigation of the impact of a local grid refinement in terms of performance and set-up.

1.4 Outline report

Chapter 2 describes the VlaBa-FM model set-up. The hydro-morphodynamics validation of the Delft3D-FM model against data and the original Delft3D-4 VlaBa model follows in Chapter 3. Chapter 4 discusses the potential of grid refinement with Delft3D-FM. Chapter 5 presents the discussion, conclusions and recommendations.

2 VlaBa-FM model set-up

2.1 Delft3D VlaBa model

The Delft3D-VlaBa model was developed by Röbke et al. (2018). It is a coupled, depth-averaged 2DH wave-flow model of the mouth of the Scheldt estuary, focusing on the coastal area between Zeebrugge and Cadzand. The grid resolution ranges from approx. 200x300 m offshore to 30x30 m near Zeebrugge harbor (Figure 2.1). Sediment transport and morphological change are only computed on the flow grid.

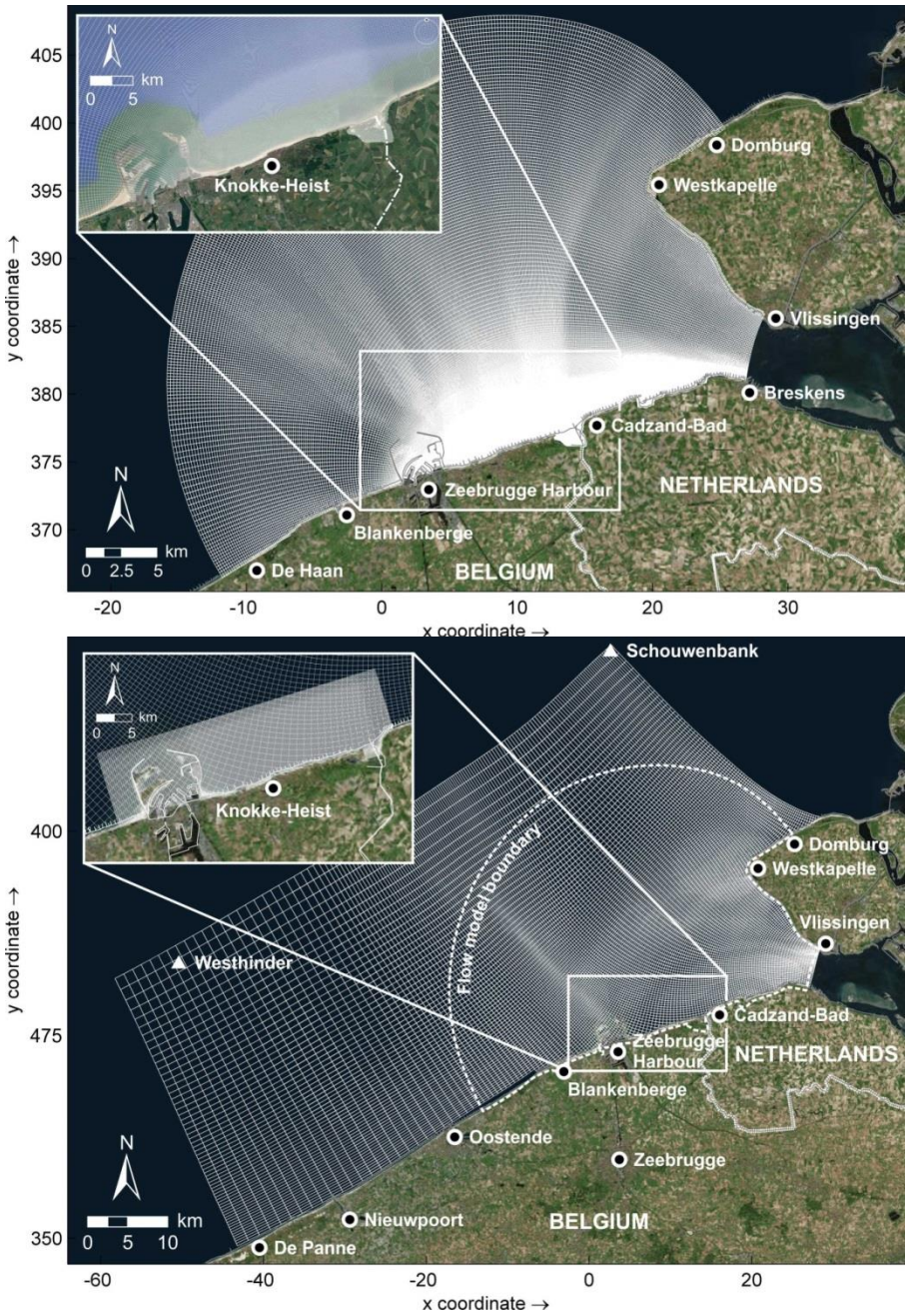

Figure 2.1 Computational grid Delft3D-VlaBa Flow (upper panel) and Wave (lower panel) model. Coordinates are given in [km] according to Amersfoort/RD New. Figure taken from Röbke et al. (2018).

The flow boundary conditions were derived from the Delft3D-NeVla model (Vroom et al. 2015). Discharges were imposed on the upstream boundary, and Riemann invariants on the downstream boundary. The latter resulted in a slightly better reproduction of flow velocities compared to offshore water level boundary conditions. The wave boundary conditions were based on the Schouwenbank and Westhinder wave data (Figure 2.2), and a uniform wind was imposed based on Vlissingen data (Figure 2.3). The Delft3D-VlaBa model accounts for salinity and associated density differences in the horizontal direction. The salinity boundary conditions were derived from the Delft3D-NeVla model as well. A discussion on the choice of these boundary conditions can be found in Röbke et al. (2018).

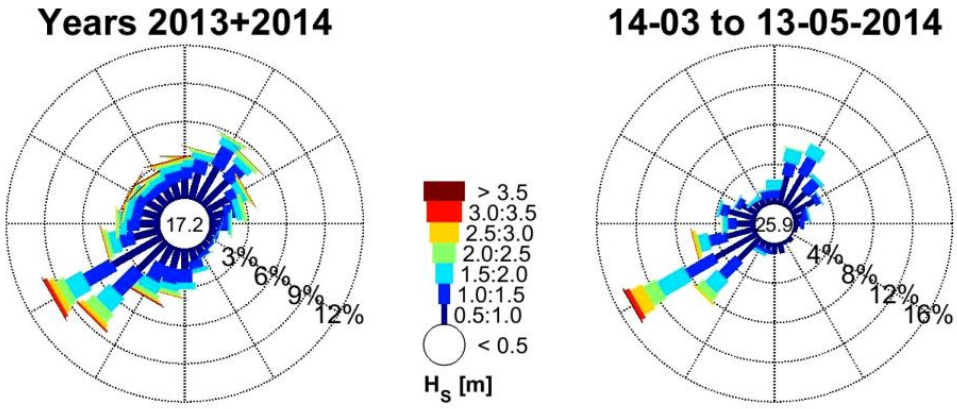

Figure 2.2 Wave roses of the years 2013+2014 and the period 14-3-2014 – 13-05-2014. The numbers in the center of both wave roses give the percentage of waves with a significant wave height Hs<0.5m. The wave climate of the 2-month period is generally in accordance with the average wave climate recorded for 2013 and 2014 and therefore assumed to be representative of the wave climate. Figure taken from Röbke et al. 2018.

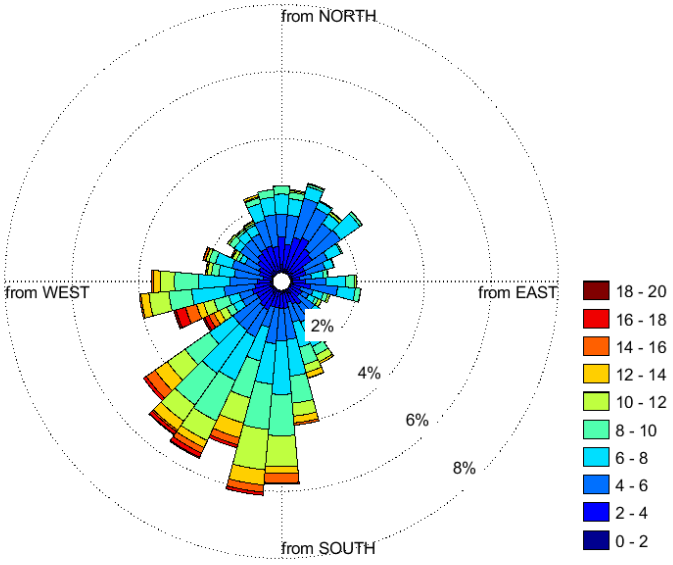

Figure 2.3 Wind rose from the station Vlissingen for the period 14-3-2014 – 13-05-2014, imposed as spatially uniform forcing.

Sediment transport was computed with the formula of Van Rijn (1993) for two sediment fractions (0.10 and 0.25 mm). The Delft3D-VlaBa accounts for non-erodible layers and spatially- and temporally-varying dredging (of navigation channel) and dumping. A morphological acceleration of 60.83 was applied to scale-up a representative 2-month period to 10 years of morphological change.

The computed water levels agree well with measurements at four locations (Zeebrugge, Cadzand, Westkapelle, Vlakte van de Raan, Figure 2.2): a bias between +0.03 and +0.09 m a uRMSE (unbiased root-mean-square error) between +0.06 and +0.08 m. A definition of the bias and uRMSE can be found in Vroom et al. (2015). A positive bias indicates an overestimation of the mean values, and a positive uRMSE an overestimation of the variation. Measured velocities at five locations (MOW3, MOW4, W7, GVW1, GVW4) were computed with a bias between -0.08 and +0.02 m/s and a uRMSE between -0.10 and +0.08 m/s (both magnitude). The calibrated Delft3D-VlaBa model reproduced the important morphological changes between 1986 and 1996. Model performance was less good for the morphologically more stable validation period between 2001 and 2011.

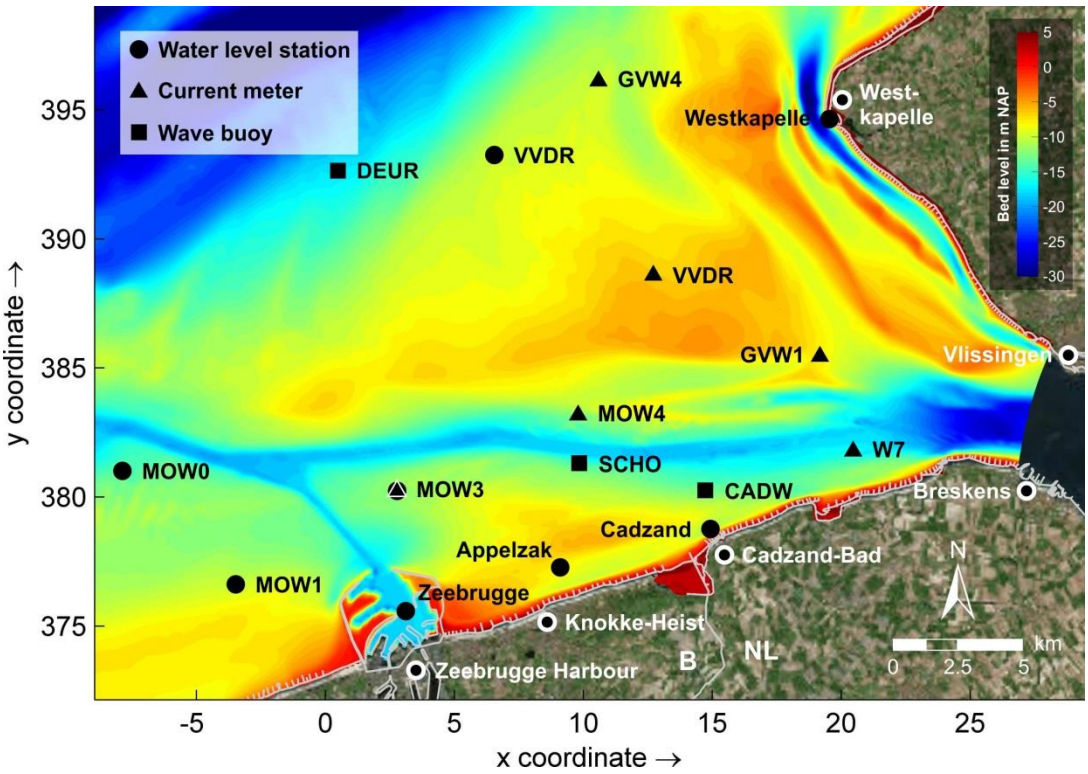

Figure 2.4 Locations of water level stations, current meters and wave buoys, the measured data at which were used for the hydrodynamic validation of the Delft3D-VlaBa model. Figure taken from Röbke et al. (2018).

We re-ran the Delft3D-VlaBa model with the initial model bathymetry defined at the cell centers (Dpsopt=DP), a uniform sediment thickness (see Section 2.2) and a boundary reflection coefficient alpha = 0 (Section 3.1.1) to enable a good comparison to the VlaBa-FM model.

2.2 VlaBa-FM model

We converted the Delft3D-4 input (run198) to a Delft3D-FM model input using the Open Earth Tools Matlab script d3d2dflowfm.m written by Theo van der Kaaij. Thereafter a few manual checks and modification were required, especially related to the definition of the boundary conditions. For example, in Delft3D-4 velocities and discharge at the boundaries are positive in the positive M- and N-direction, whereas in Delft3D-FM inflow at the boundary is defined as positive. The treatment of the boundary locations is different in Delft3D-4 and Delft3D-FM. In Delft3D-4 the boundary locations are defined per M,N-segment and in Delft3D-FM per location. The automated conversion resulted

in 36 Delft3D-FM boundary support points and 36 discharge time-series for the 18 Delft3D boundary segments. We modified this to 18 pairs of boundary support point and 18 discharge time-series.

Also, the way Riemann type boundary conditions are taken care of is different in Delft3D-4 and Delft3D-FM. In Delft3D-4 the Riemann invariant, R [m/s], at the boundary (positive sign being into the domain) is:

$$R = U + 2\sqrt{gH} = U + 2\sqrt{g\left(d+\zeta\right)} \approx U + 2\sqrt{gd} + \zeta\sqrt{\frac{g}{d}} \qquad (0.1)$$

provided $|\zeta|/d << 1$. Here *g* is the gravitational acceleration, *H* the water depth, *d* the depth below reference level (*z* = 0 m), and ζ the water level. The first and third term on the right-hand side of Eq. (2.1) should be imposed, the second term is computed from the model bathymetry. This Riemann option is not (yet) available in Delft3D-FM. Instead, the Riemann invariants are rewritten to water levels [m] and only the water level at the boundary needs to be prescribed. As it was unclear how to transform the Delft3D-4 Riemann invariants [m/s] to Delft3D-FM Riemann water levels [m], how Riemann boundary conditions are taken care of exactly in Delft3D-FM and preliminary tests were unsuccessful, we decided to continue with water level type of boundary conditions.

In Delft3D-4 the thickness of the available bed sediment is defined in the grid cell centre (SDB-files). In Delft3D-FM the sediment thickness should overlap the grid, so the XYZ-files derived from the original SDB-files were spatially extended. We chose for a uniform sediment thickness in the VlaBa-FM model runs.

The Delft3D-4 VlaBa model runs were modified to have identical model settings to the Delft3D-FM settings to ensure a fair comparison of Delft3D-FM with Delft3D-4 results, see Table 2.1.

Table 2.1 Parameter settings of the Delft3D-Vlaba model

Parameter	Setting
Friction coefficient Manning [$s/m^{1/3}$]	0.02
Vicouv [m^2/s]	1
Dicouv [m^2/s]	0.1
Smagorinsky [-]	0
Sus [-]	0.3
Bed [-]	0.1
SusW [-]	0.05
BedW [-]	0.05

2.3 Model runs

This project of the conversion of the Delft3D-4 VlaBa model to Delft3D-FM spanned a period of 1.5 years. Therefore, not all simulations discussed here were performed with an equal software version. Keeping up with the newly released software versions helped the identification of software limitations. The calculations discussed in Chapter 3 were carried out with Delft3D-FM version 2.02.07_59215 (19 November 2018), see Table 2.2. Grid refinement capabilities are discussed in Chapter 4 and were computed with Delft3D-FM version 2.10.05_65238 (10 January 2020), see Table 2.3.
All simulations were run on the Deltares h6 quad-core Unix cluster. The tide-only hydrodynamic simulations cover the complete year of 2014. The morphological simulations (incl. waves and dredging and dumping) were carried out for the same 2-month representative period as the original

Delft3D-4 simulations, March 14th, 2014 to May 13th, 2014, with different morphological acceleration factors. Parallelization of the simulations was investigated to reduce computational times.

Table 2.2 Overview of reported simulations in Chapter 3 with FM-model version 2.02.07_59215.

runid	Model	Period	Mor	Morfac	DAD	Domains
1	Delft3D4	2014	N	N/A	N	1
2	Delft3D4	14/03-13/05 2014	Y	1	N	1
3	Delft3D4	14/03-13/05 2014	Y	60.82	N	1
4	Delft3D4	14/03-13/05 2014	Y	60.82	Y	1
5	Delft3D-FM	2014	N	N/A	N	1
6	Delft3D-FM	14/03-13/05 2014	Y	1	N	1
7	Delft3D-FM	14/03-13/05 2014	Y	60.82	N	1
8	Delft3D-FM	14/03-13/05 2014	Y	60.82	Y	1
9	Delft3D-FM	14/03-13/05 2014	Y	60.82	Y	4
10	Delft3D-FM	14/03-13/05 2014	Y	60.82	Y	8

Table 2.3 Overview of reported simulations in Chapter 3 with FM-model version 2.10.05_65238.

runid	Model	What?	Mor	Morfac	DAD	Domains
D3D01	Delft3D4	Base grid	Y	60.82	Y	1
D3D02	Delft3D4	Base grid, scenario	Y	60.82	Y	1
FM01	Delft3D-FM	Base grid	Y	60.82	Y	8
FM02	Delft3D-FM	Base grid, scenario	Y	60.82	Y	8
FM03	Delft3D-FM	Refined grid	Y	60.82	Y	8
FM04	Delft3D-FM	Refined grid, scenario	Y	60.82	Y	8

3 VlaBa-FM model validation

The VlaBa-FM model results are benchmarked against the Delft3D-4 results in this chapter. First, we compared the hydrodynamics during the representative period March 2014 – May 2014 between the two models as well as referenced to observations in a morphostatic computation. After that, we turned morphodynamics on and we compared bed levels and dredged volumes. A last step we took was a validation of the scalability of parallelization of the computation.

3.1 Hydrodynamics

3.1.1 Water levels

Figure 3.1 and Figure 3.2 compare the observed and computed amplitudes and phases of the M2 and S2 tidal components for April 2014 (for the location of the stations see Figure 2.4). It includes Delft3D-FM model results and two Delft3D-4 model results, with different values of the boundary reflection coefficient alpha. In the original Delft3D-4 VlaBa model alpha = 400 s^2, to reduce the reflection of outgoing waves at the boundaries.

Although not negligible, the effect of the reflection coefficient on the computed tidal amplitudes is small. A positive reflection coefficient increases the phase of the Delft3D-4 simulation, which leads to a reduction of the propagation of the tidal wave. It is not (yet) possible to impose an alpha value on the Delft3D-FM model boundary. The Delft3D-FM-computed phases agree well with the Delft3D-4 model results with alpha = 0 s^2. Both show a better match with the observed phases than the Delft3D-4 model with alpha = 400 s^2. Therefore, the following Delft3D-4 model results are based on simulations with alpha = 0 s^2.

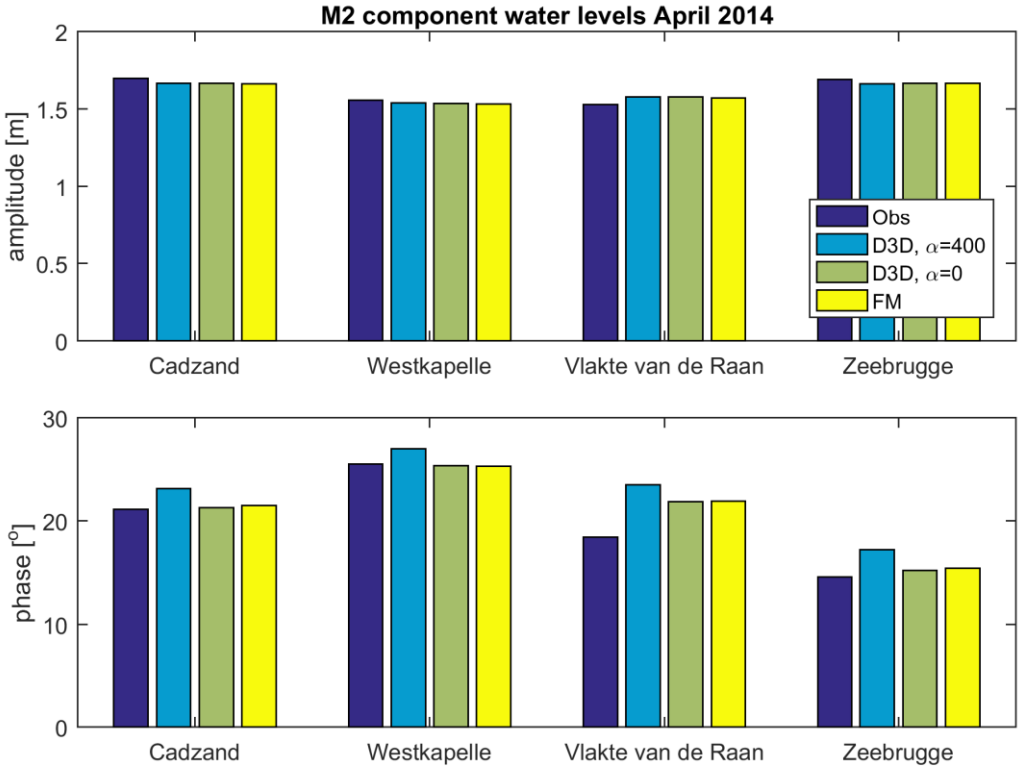

Figure 3.1 Comparison between the observed and computed amplitude and phase of the M2 tidal water level component (April 2014). It includes Delft3D-4 model results with different values of reflection coefficient alpha, and Delft3D-FM model results.

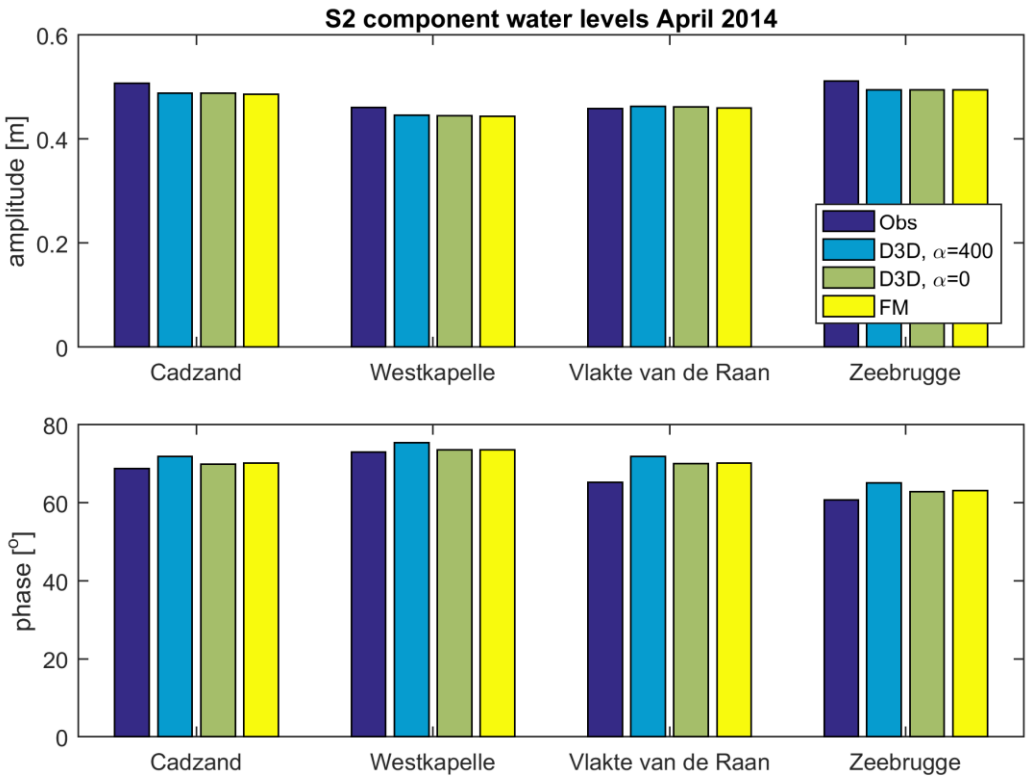

Figure 3.2 Comparison between the observed and computed amplitude and phase of the S2 tidal water level component (April 2014). It includes Delft3D-4 model results with different values of reflection coefficient alpha, and Delft3D-FM model results

3.1.2 Flow velocities

Figure 3.3 and Figure 3.4 compare observed and computed depth-averaged flow velocities in August/September 2014 (for the location of the stations see Figure 2.4). The Delft3D-4 and Delft3D-FM velocities are comparable. The root-mean-square-errors (RMSE) never differ more than 0.02 m/s and range ranging 0.06 m/s to 0.14 m/s over the observation stations. The RMSE phases range 11° to 16°. These are considered good, and in both Delft3D-4 and Delft3D-FM are caused by a mild underestimation of peak tidal velocities.

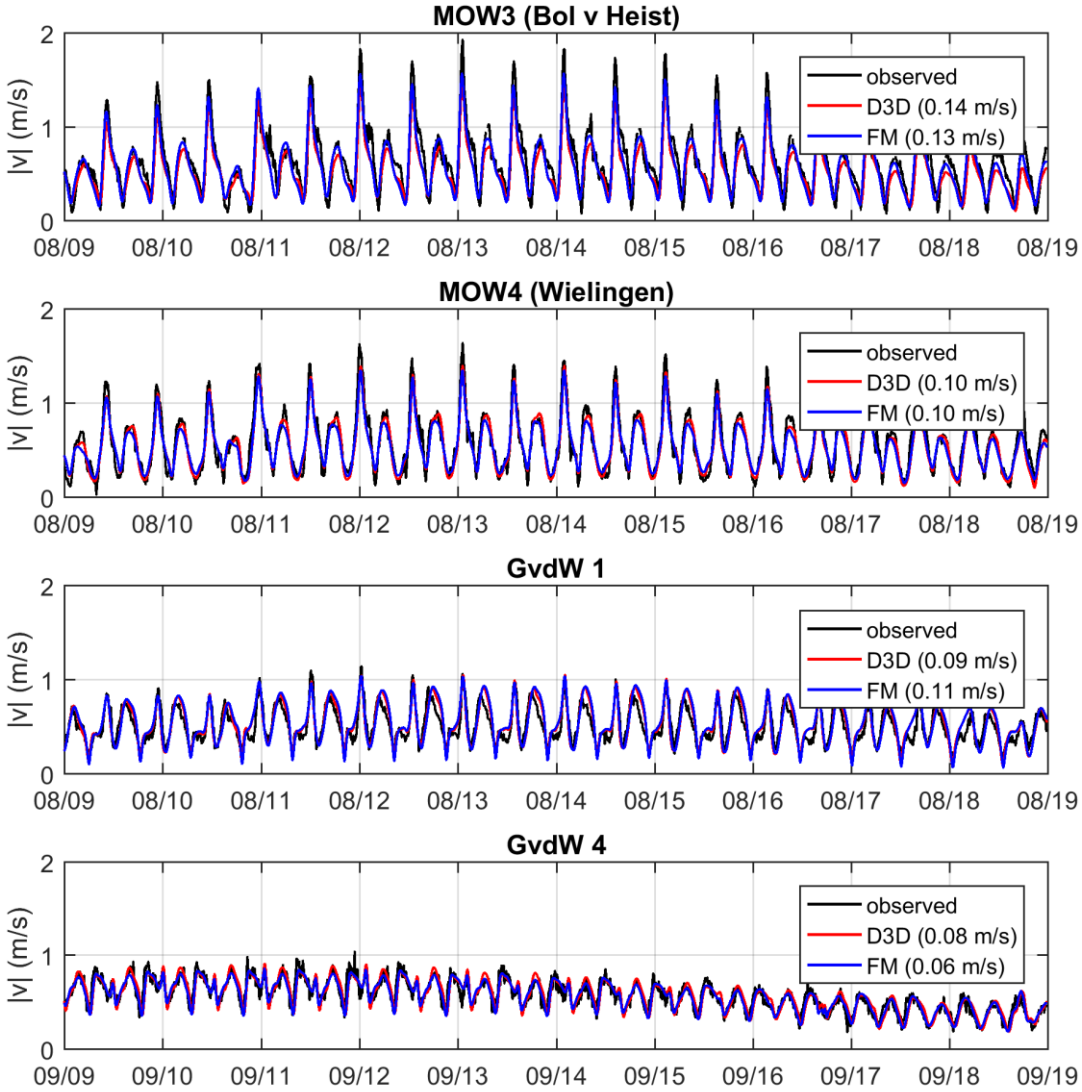

Figure 3.3 Comparison between the observed and computed depth-averaged velocity magnitudes in August/September 2014. The RMSE-values are given between brackets.

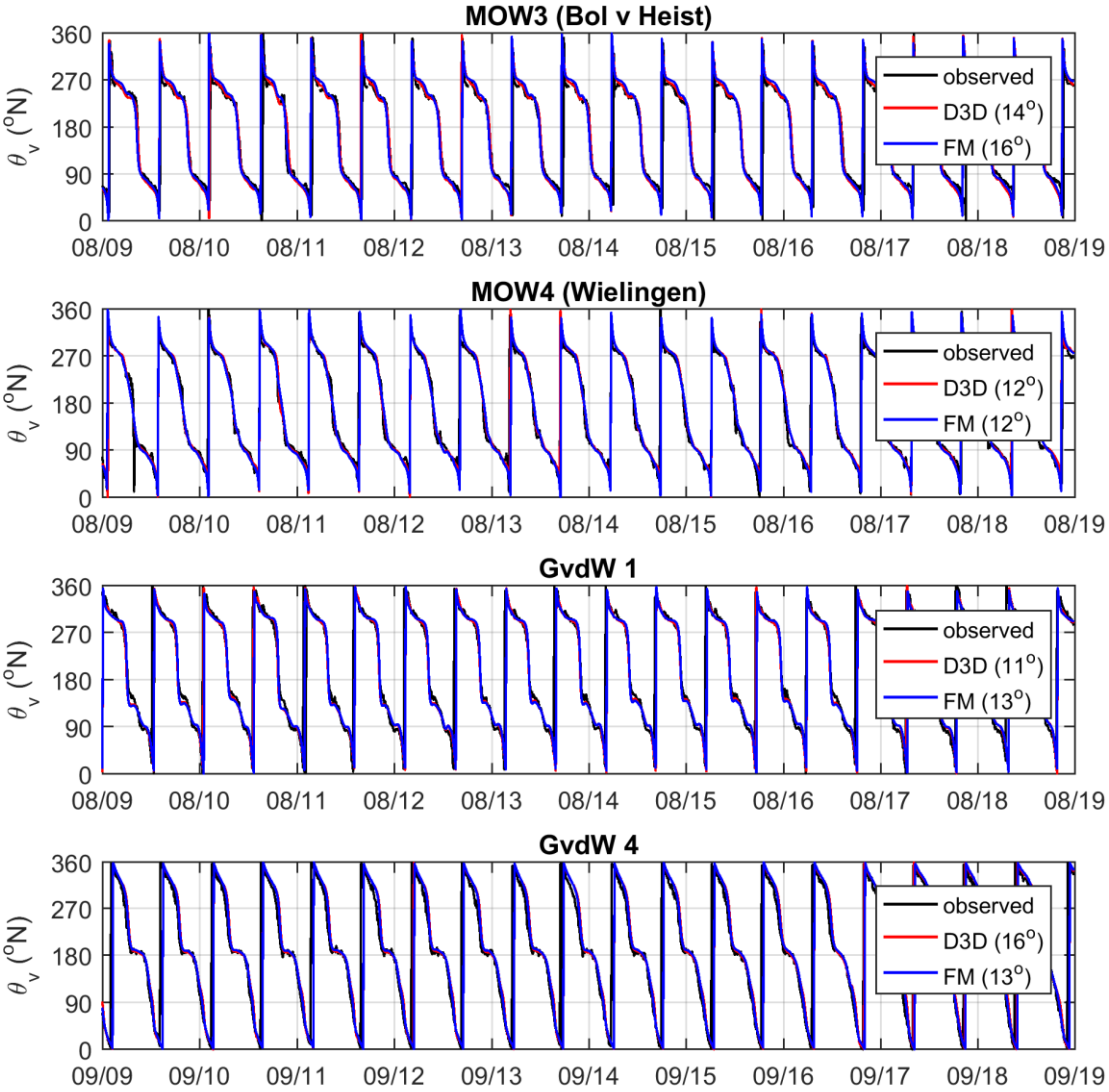

Figure 3.4 Comparison between the observed and computed depth-averaged phases in August/September 2014. The RMSE-values are given between brackets.

3.1.3 Wave heights

Wave propagation is modelled through the wave action equation that is solved with the SWAN model and then coupled to the flow model to account for a two-way coupling between waves and currents. The SWAN model did not change between the coupling with Delft3D-4 and Delft3D-FM. Any differences in results can therefore only be a result of wave-current-interaction. We compared the significant wave heights at four observations stations between Delft3D-4 and Delft3D-FM in Figure 3.5 with observed timeseries for reference. The RMSE difference between observations and model is equal for the Delft3D-4 and Delft3D-FM results and varies between 0.15 m/s and 0.2 m/s. A small discrepancy between the Delft3D-4 and Delft3D-FM result is only identified at station CAWI. It can therefore be concluded that the minor differences in flow velocities did not amplify in the significant wave height field.

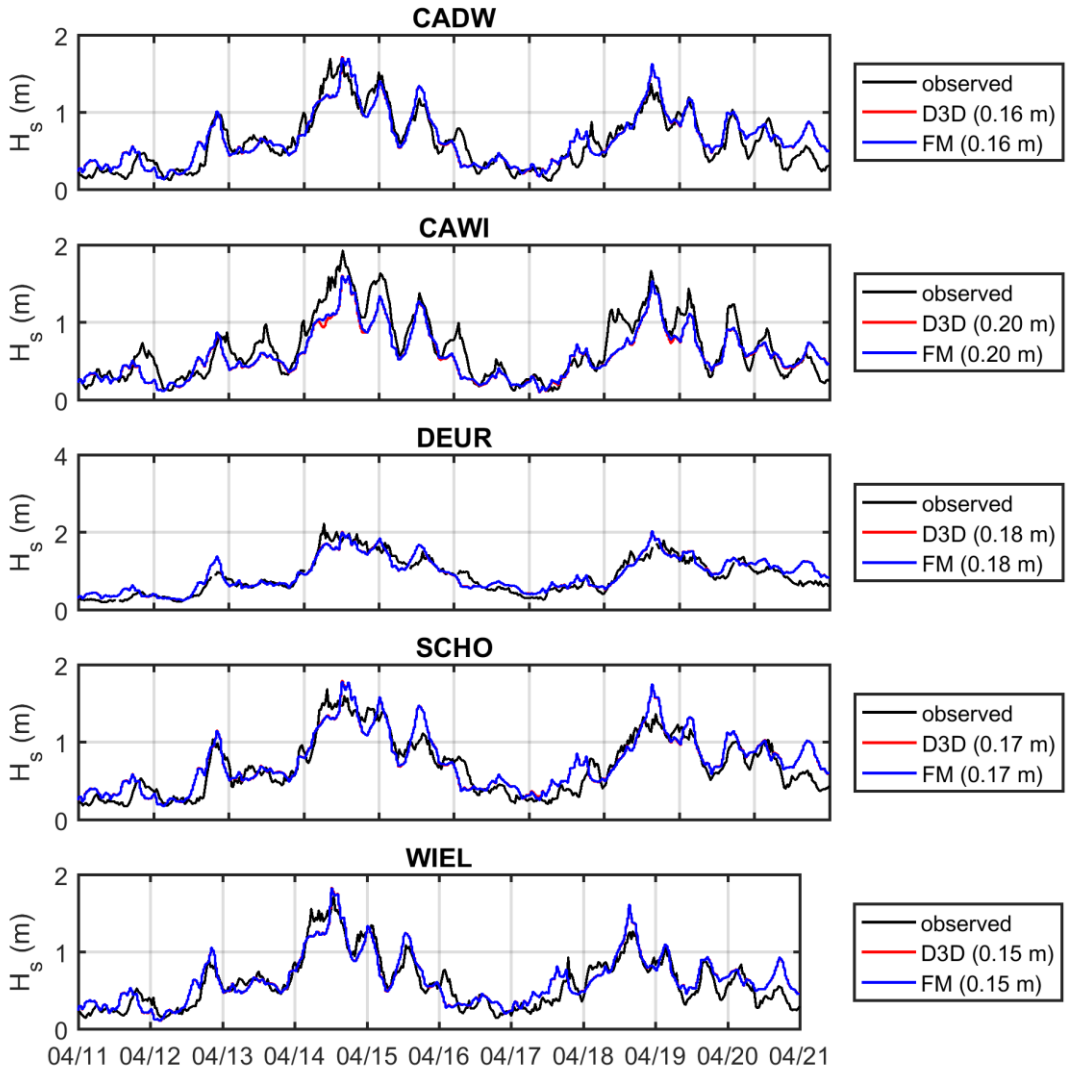

Figure 3.5 Comparison between the observed and computed depth-averaged significant wave heights in April 2014. The RMSE-values are given between brackets.

3.2 Morphodynamics

3.2.1 Bed levels

We build up the morphodynamic computations with increasing complexity, starting with a morphodynamic run without dredging and dumping and a morphodynamic timescale equal to the hydrodynamic timescale (MorFac=1), see Figure 3.6. General patterns are very similar between Delft3D-4 and Delft3D-FM. Small differences can be identified along the coast between Westkappelle and Domburg, but at the focal area of the navigational channels and the harbour the patterns compare well.

The overall patterns of erosion and sedimentation remain similar but increase in magnitude when the morphological acceleration factor is increased, such that the simulation represents 10 years of morphodynamics. The small differences identified between Westkappelle and Domburg diminish in these simulations with MorFac 60.82, see Figure 3.7.

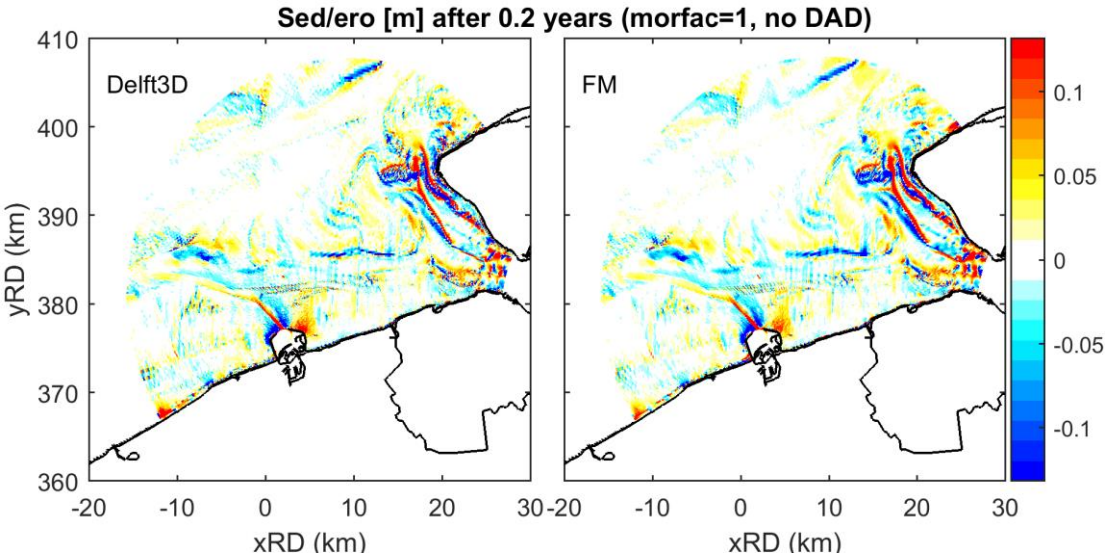

Figure 3.6 Comparison of final bed levels with MorFac = 1, no dredging and dumping and no domain-decompositioning

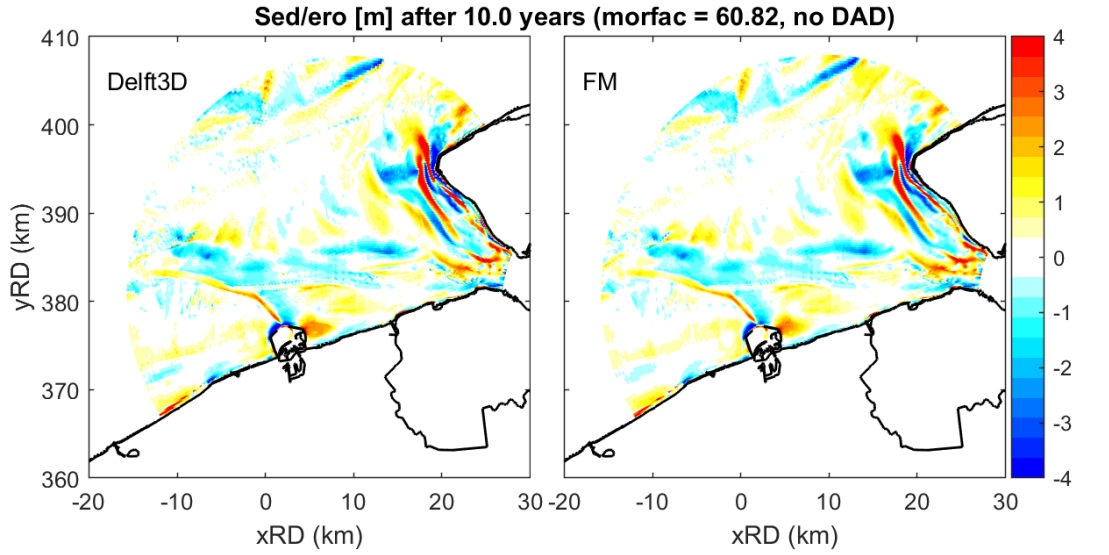

Figure 3.7 Comparison of final bed levels with MorFac = 60.82, no dredging and dumping and no domain-decompositioning

A time-dependent dredging-and-dumping algorithm instantly removes sediment from the bed if the bed level exceeds a prescribed dredge depth and places this excess sediment layer on top of the bed of the dump location. The dump locations are clearly visible in the final erosion-sedimentation pattern, because of this direct implementation of the dumping in the bed layer instead of in the water column at the dump location, see Figure 3.8. Again, the general erosion-sedimentation patterns compare well between Delft3D-4 and Delft3D-FM.

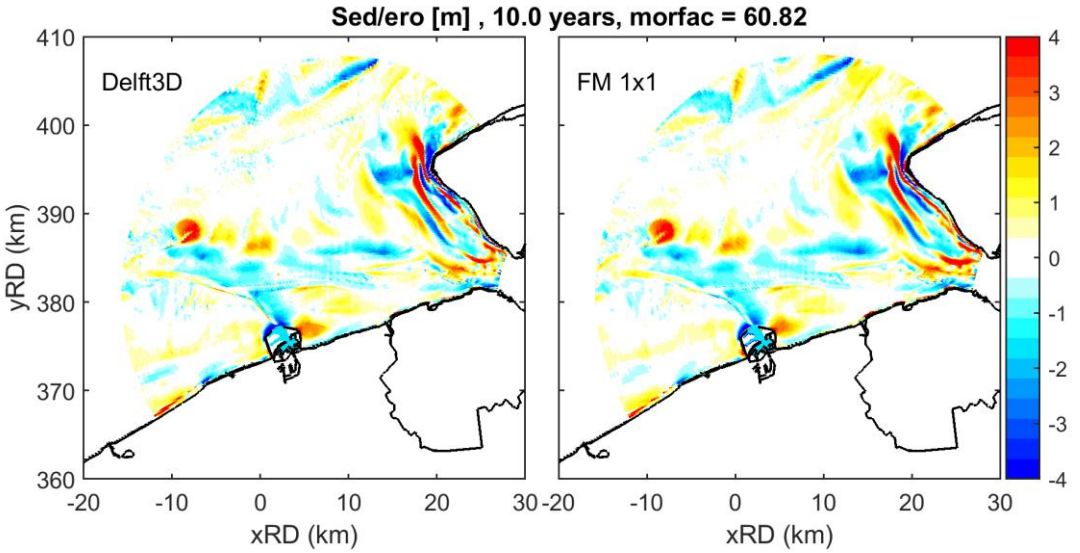

Figure 3.8 Comparison of final bed levels with MorFac = 60.82, with dredging and dumping, computation without domain-decompositioning.

The final check on erosion/sedimentation is plotted in Figure 3.9, where the change of mass availability in the bed, differentiated between the two sediment fractions, is compared between Delft3D-4 and Delft3D-FM. Similar to the total bed level change, the erosion/sedimentation of the two sediment fractions compares well between the two models.

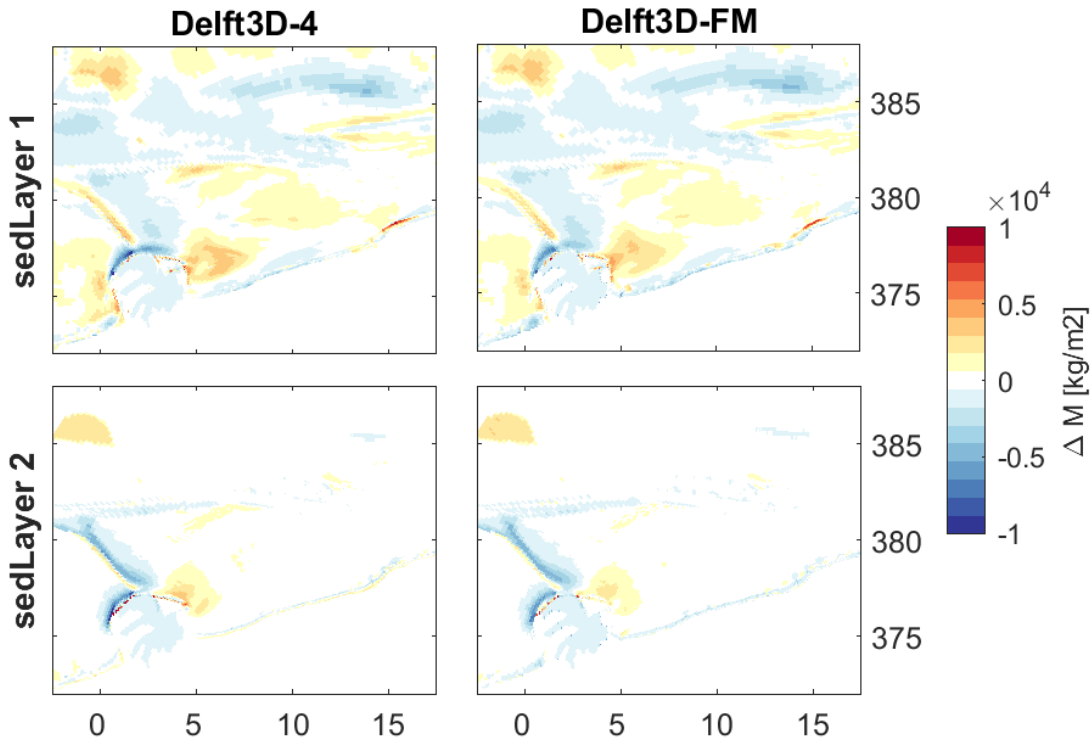

Figure 3.9 Comparison of total change of mass availability in the bed between the Delft3D-4 computation and Delft3D-FM for the two sediment fractions (D50 of 0.1 and 0.25 mm). MorFac=60.82, with dredging and dumping.

Figure 3.6 - Figure 3.9 summarize the bed level changes of the entire domain. Four timeseries of bed levels at observation stations are plotted in Figure 3.10 to quantify more clearly local differences in bed levels between Delft3D-4 and Delft3D-FM. At Wielingen and Scheur 3, the actual bed level lies below the prescribed dredge depth throughout the entire simulation and is therefore updated freely as the Exner equation prescribes. Small differences between the bed levels in the Delft3D-4 and Delft3D-FM simulation are observed up to 20 cm. In both models the bottom is observed to clearly breathe with the tide as a consequence of the large morphological acceleration factor. At the Pas van het Zand (PvZ2) the prescribed dredge depth is reached in the first morphological year due to sedimentation. After this moment, the bed level is prescribed by the dredge depth correctly in both models. At Open boundary 8 (located on the edge of the main dump site), the free evolution of the bed is similar between the two models for the first 3 years. Differences start occurring between Delft3D-4 and Delft3D-FM bed levels after that and increase over time. This is attributed to an accumulation of differences in dredged sediments that grows over time.

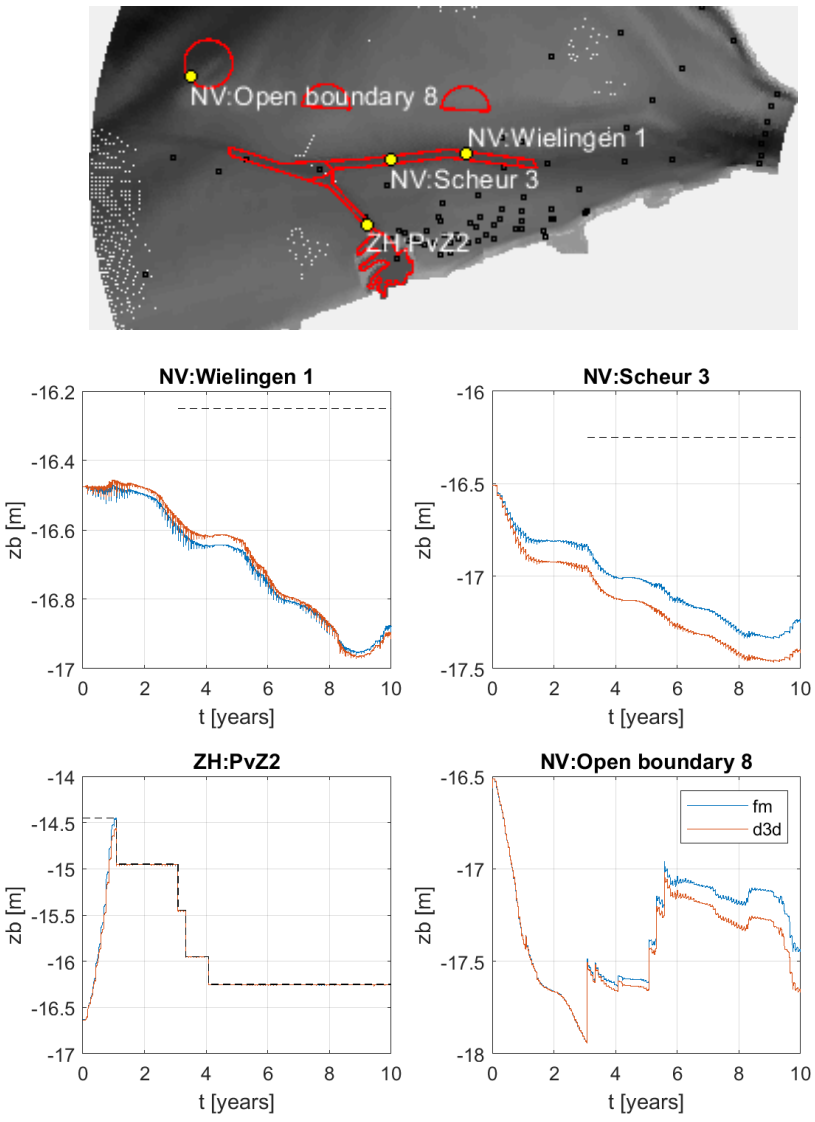

Figure 3.10 Comparison of timeseries of bed level at four stations in dredge or dump areas (indicated in yellow on the reference figure. The dashed black line indicates the time-varying dredge depth at the respective observation station location.

3.2.2 Dredging and dumping

A comparison of cumulative dredged sediments of four dredge areas are plotted in Figure 3.11. At these locations the dredged sediments in the Delft3D- FM simulations are typically 10% higher than in the Delft3D-4 simulations. This is in line with a higher bed level in the Delft3D-FM simulation at Open Boundary 8 (Figure 3.10).

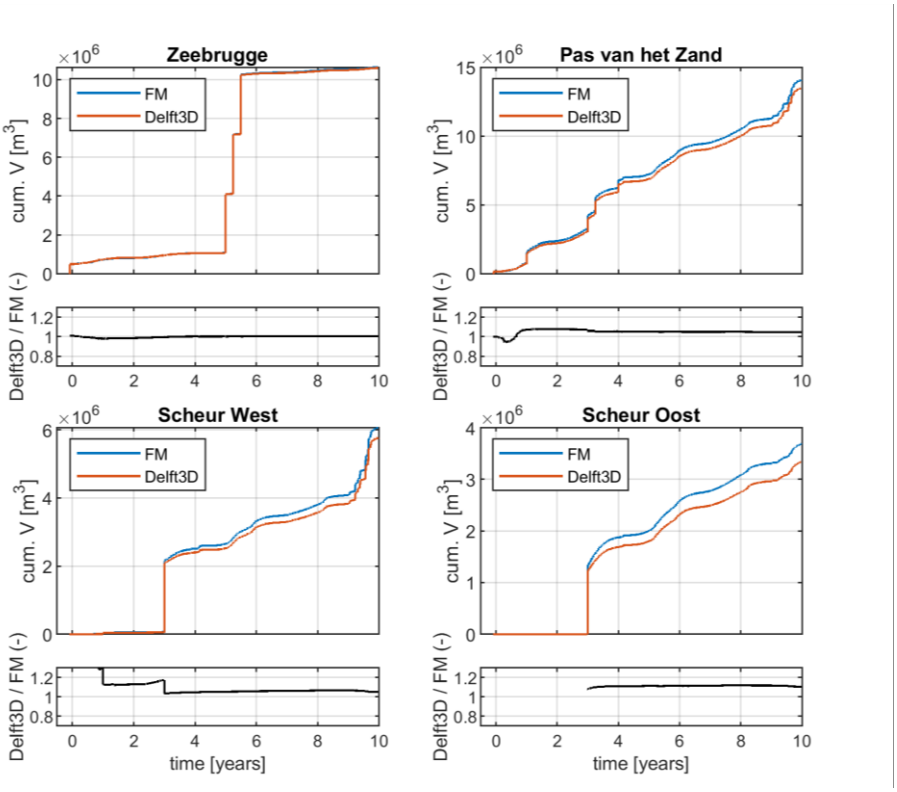

Figure 3.11 Comparison of cumulative dredged volumes of four dredged areas (top panels) and the ratio between the dredged volumes in Delft3D-4 and Delft3D-FM (bottom panels). See Figure 2.4 for reference of locations of dredge areas.

3.3 Parallel computing

3.3.1 Domain partitioning

All Delft3D-FM model simulations discussed until here have been computed on a single machine without domain partitioning. The computation is distributed over the processors of this machine with the OpenMP (*Open Multi-Processing*) protocol. OpenMP speeds up calculations by employing multiple processor cores in a single (shared-memory) computer.

OpenMP-parallelism in Delft3D-FM does not scale as well as MPI-parallelism (*Message Passing Interface system*). MPI can be run both on computing clusters with distributed memory as well as shared memory machines with multiple processors and/or multiple CPU cores. Therefore, Delft3D-FM switches to the MPI protocol for the FLOW computation in case more than one machine is deployed. With this protocol, the computational domain needs to be partitioned into as many subdomains as processors involved. These subdomains overlap slightly and every timestep the results on these overlapping areas are communicated.

There are automatic partitioning algorithms, such as the METIS partitioner that optimally partitions into domains with comparable number of grid cells and minimalization of subdomain boundary length. A partitioning of the current FLOW domain with the METIS algorithm into 8 domains is plotted in Figure 3.12 (left panel). Several dredge or dump sites are crossed by subdomain boundaries in

this partitioning. Although planned as future capability, dredging and dumping on subdomain boundaries is not yet a properly working functionality in Delft3D-FM.

To be able to parallelize the computation over more than one machine regardless, it is also possible to define a manual partitioning (see Figure 3.12 right panel). The distribution of grid cells over the subdomains is less optimal in this partitioning, but more importantly no subdomain boundaries cross dredge or dump sites. With this partitioning, the erosion-sedimentation pattern as computed with Delft3D-FM on 2 machines with each 4 cores shows a comparable sedimentation-erosion pattern as the Delft3D-4 simulation (Figure 3.13).

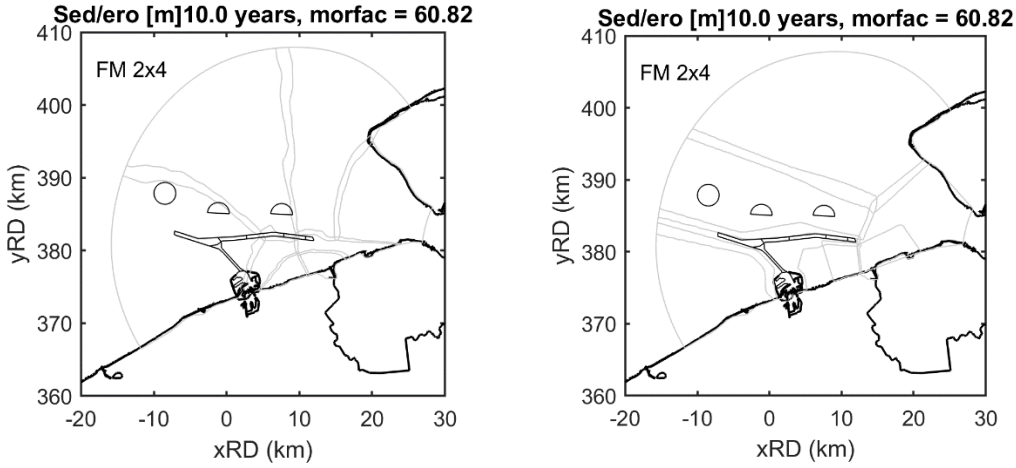

Figure 3.12 Domain decomposition into 8 domains (light grey lines) with dredge and dump areas for reference (solid lines) with METIS partitioner (left); with a manual decompositioning that avoids splitting dredge and dump areas (right).

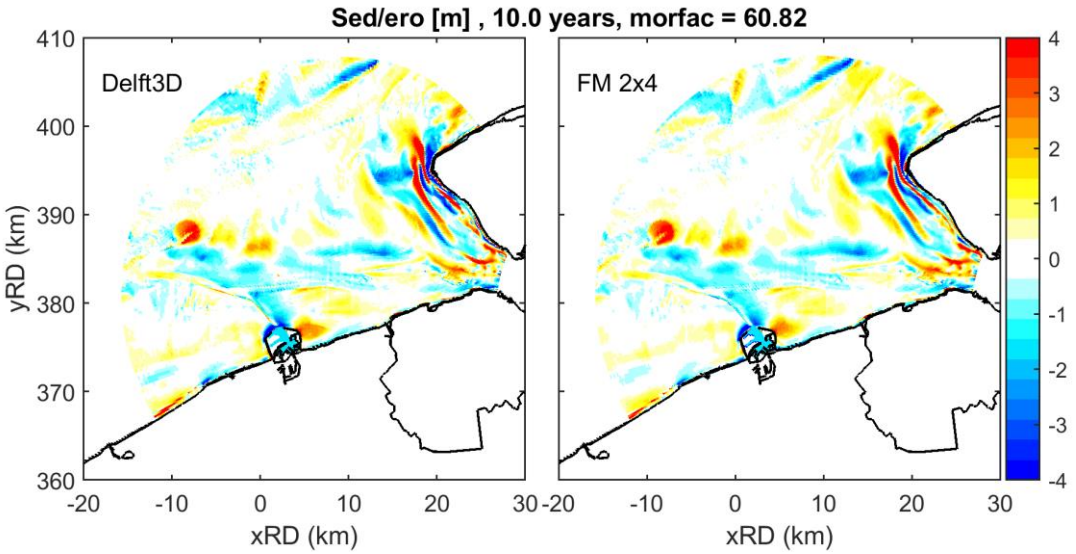

Figure 3.13 Comparison of final bed levels with MorFac = 60.82, with dredging and dumping, serial computation of waves and parallelization of the flow computation over 8 domains (2 nodes with each 4 cores).

3.3.2 Computational efficiency

Parallelization of the computation is intended to speed up the computational time of the simulation. The original Delft3D-4 simulation took 92 hours of computational time on the Deltares H6-normal-e3-cluster on one virtual machine for 10 years of morphology. The Delft3D-FM simulation without domain decompositioning is faster at 70 hours (Table 3.1). This is largely attributed to an, on

average, larger timestep possible in Delft3D-FM than in Delft3D-4. In Delft3D-4 the numerical method is implicit, such that the user can define a time step herself. This time step needs to be representative for the time scale of the processes she aims to resolve. The default timestep in Deflt3D-FM is Courant-limited, and hence depends on grid resolution and flow velocities. The timestep is updated every computational timestep based on the hydrodynamic Courant conditions.

With domain partitioning of the FLOW domain, this can be sped up further to 49 hours on 4 domains, or 46 hours on 8 partitions. Although with 8 partitions the computational time for the FLOW computation is reduced from 21 to 13 hours, the WAVE simulation is taking more time (28 to 33 hours). Since the WAVE grid is not partitioned yet, and therefore is completely computed on one processor, no speed up is expected with increasing partitions of the FLOW computation. The increase of time taken for the WAVE computation is hypothesized to be caused by increased communication time from the WAVE computation to the extra FLOW partitions. For this particular model, the efficiency of the parallelization is constrained by the WAVE computation, and it is therefore fruitless to partition the FLOW grid into more than 8 subdomains.
Decompositioning of the WAVE simulation is hoped to improve the scalability of the computational time of the current model in the foreseeable future. With the current state of the model, a speed up of 2x is reached in comparison with the reference Delft3D-4 model, at the expense of an extra virtual machine for the computation.

Table 3.1 Computational time with various parallelization techniques for 10 years of morphodynamics with a MorFac of 60.82

	Partitions	Type of parallelization	Machines	Partitions per machine	Flow (Hr)	Wave (Hr)	Total (Hr)
Delft3D-4	1	OpenMP	1	4	67	26	93
Delft3D-FM	1	OpenMP	1	1	49	21	70
Delft3D-FM	4	MPI	2	2	21	28	49
Delft3D-FM	8	MPI	2	4	13	33	46

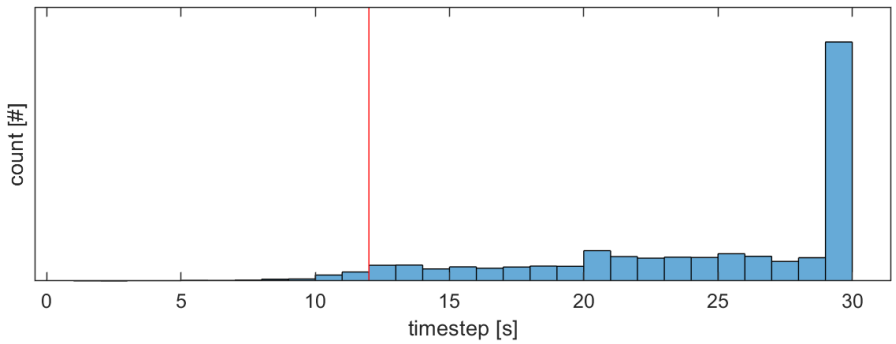

Figure 3.14 Histogram of the timestep in Delft3D-FM (blue) and the constant timestep used in Delft3D-4 (red line) for reference.

4 Grid refinement

Delft3D-FM is set up to work with unstructured meshes, which may by truly unstructured or may be an unstructured representation of a quadrilateral (e.g. curvilinear) grid. This makes the refinement criteria less strict than applied in Delft3D4 and allows local grid refinement. We use the VlaBa model to show the potential of this local grid refinement at an artificial island between Zeebrugge and Cadzand and to validate the results on a refined mesh.

4.1 Refinement criteria

The unstructured mesh to be used in Delft3D-FM can consist of cells with 3-6 vertices, where mixing of cell-shapes is possible. Currently, the recommended approach is to use quadrilaterals as much as possible and use triangles for connecting grids. An unstructured grid needs to comply to two criteria:

1. Orthogonality of the cell-links,
2. Smoothness of transitions in cell area.

Consequently, a local refinement works best if the refinement boundaries are chosen such that they respect the directionality of the coarser base grid. E.g. a polygon defining the refinement should intersect the coarse grid's vertices as orthogonally as possible. This minimizes the number of cells affected by the connection between coarse and refined grid. If the refinement polygon crosses quadrilaterals exactly orthogonal, only one row of connecting cells is required, see Figure 4.1. If coarse grid cells are crossed diagonally by the refinement polygon, a larger area of cells will require reorientation of its vertices to comply with orthogonality criteria.

With a coded, or manually drawn refinement polygon the Delft3D-FM suite has automated tools to connect the local grid refinement to the base grid. The preferred method for generating the connectivity between refined and base grid with a minimal amount of connecting cells is the Casulli method. With this method the grid is refined a factor two in both horizontal directions and the connection to the base-grid occurs with triangles and trapezoids (Figure 4.1).

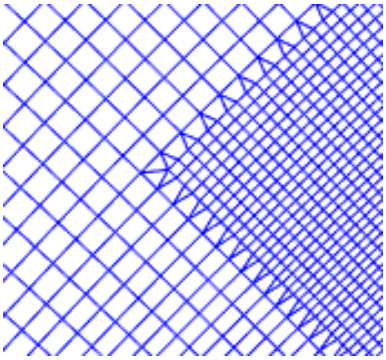

Figure 4.1 Casulli-type connectivity of the refined area and the base grid

4.2 Case study: pilot-island

The VlaBa grid was designed for mid-term (i.e. 10 years) morphological computations. Therefore, the grid resolution was a trade-off between resolution where it matters (along the beaches of Cadzand) and model-size (going coarse offshore) for the sake of computational time. Sufficient resolution is needed for resolving complex geometries such as harbour inlets, and around the wave breaking zone. The current VlaBa grid has sufficient resolution. To add a resolution criterium in order to test the grid-refinement capabilities of Delft3D-FM, the pilot-island scenario schematisation has been revisited. The pilot-island scenario places the breaker zone further offshore, as the waves will

break on the upwind shore of the artificial island. Because the original VlaBa grid get coarser in offshore direction, a local grid refinement would be desired around the island heads. The pilot-island scenario does not represent any current ideas in the Vlaamse Kustvisie anymore, and in this report only serves as a test-case for grid refinement.

To minimize the required number of cells to transition from the base grid to the local refinement, a refinement area has been chosen that respects the base grid's cell orientation and alignment. Ignoring this grid orientation led to large areas of reorientation of cell vertices in in the base grid, because the orthogonality criterium was severely violated. Therefore, a refinement area was chosen with orthogonal edges (Figure 4.2). The grid was refined by a factor two in both directions.

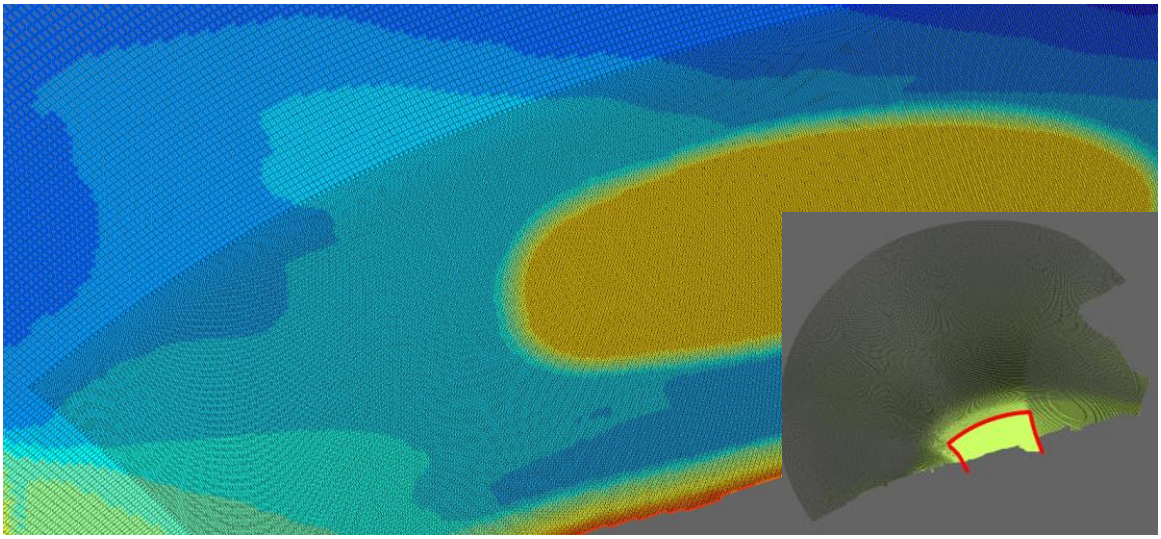

Figure 4.2 Computational grid (black lines) with colors indicating depth for reference. The inset figure shows the extent of the refinement area indicated with a red line.

4.2.1 Scenario lay-out

10 years of morphological change around the pilot-island is investigated using this scenario model. The hydrodynamic forcing to represent these 10 years is the same timeseries as for the model discussed in Chapter 3, taken from two months in Spring 2014. The dredge-and-dump scenario as discussed in Vroom et al. (2016) is applied. Unlike the validation-scenario 1986, this is a continuous and unchanged scenario for the entire 10 years.

The scenario's initial bathymetry is based on the 2011 bathymetry (Röbke et al. 2018) in which an artificial island is constructed with a height of 2.5m+NAP at the Paardenmarkt (Figure 4.3). Unlike the the model discussed in Chapter 3, the pilot-island-scenario model prescribes a spatially varying finite sediment availability at the bed for both sediment fractions (D50 of 100 and 250 micrometer) (Röbke et al. 2018).

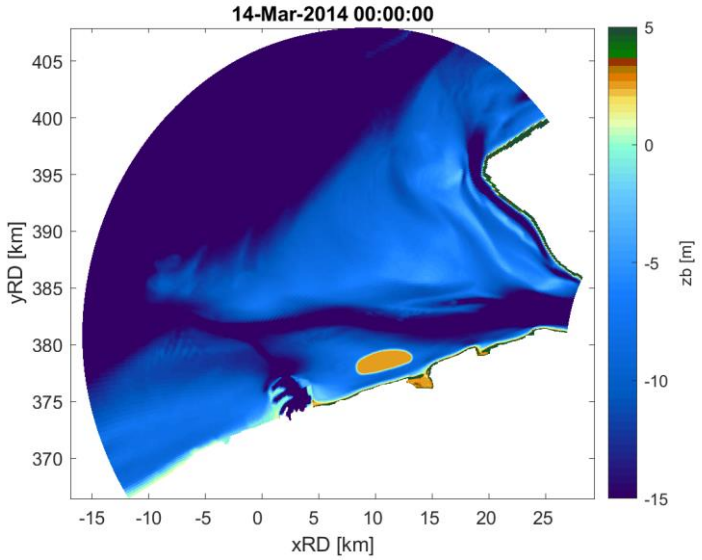

Figure 4.3 Initial bathymetry of the scenario, which is based on the 2011 bathymetry (Röbke et al. 2018) and an artificial island at 2.5m+NAP at the Paardenmarkt.

Because the initial bathymetry, sediment availability and dredge-and-dump scenario in the scenario model are different from the base VlaBa model comparison, a set of simulations was performed:

Table 4.1 Simulations discussed in chapter 4

	Description
D3D01	Delft3D-4 reference computation: standard VlaBa grid without pilot-island
D3D02	Delft3D-4 standard VlaBa grid with pilot-island
FM01	Delft3D-FM reference computation: standard VlaBa grid without pilot-island
FM02	Delft3D-FM reference computation: standard Vlaba grid with pilot-island
FM03	Delft3D-FM local grid refinement without pilot-island
FM04	Delft3D-FM local grid refinement with pilo-island

With these simulations, an additional check on comparability of Delft3D-4 and Delft3D-FM results is made, and grid refinement is tested in Delft3D-FM on the pilot-island scenario.

4.2.2 Erosion/sedimentation

A zoom of the 10-year erosion/sedimentation patterns for all simulations including the pilot-island is plotted in Figure 4.4. Patterns between Delft3D-4 and Delft3D-FM match well in the reference simulations. Because the dominant transport direction is West to East, the west-side of the pilot-island shows strong erosion and the eastward tail shows sedimentation. The depositional area in the shadow zone of the Zeebrugge harbour gets stronger. Deposition along the beaches behind the pilot-island also appears, but the channel between the pilot-island and the beaches undergo stronger erosion. Simulation FM04, with local grid refinement, gives more resolution around the pilot island. The overall erosion/sedimentation pattern is unchanged, but the depositional areas are a little better resolved. This is clearest on the East- and West tail of the pilot-island.

Neither the border of the local refinement nor the domain-decomposition boundaries can be traced back in the final erosion/sedimentation map (Figure 4.4), which is the expect behaviour.

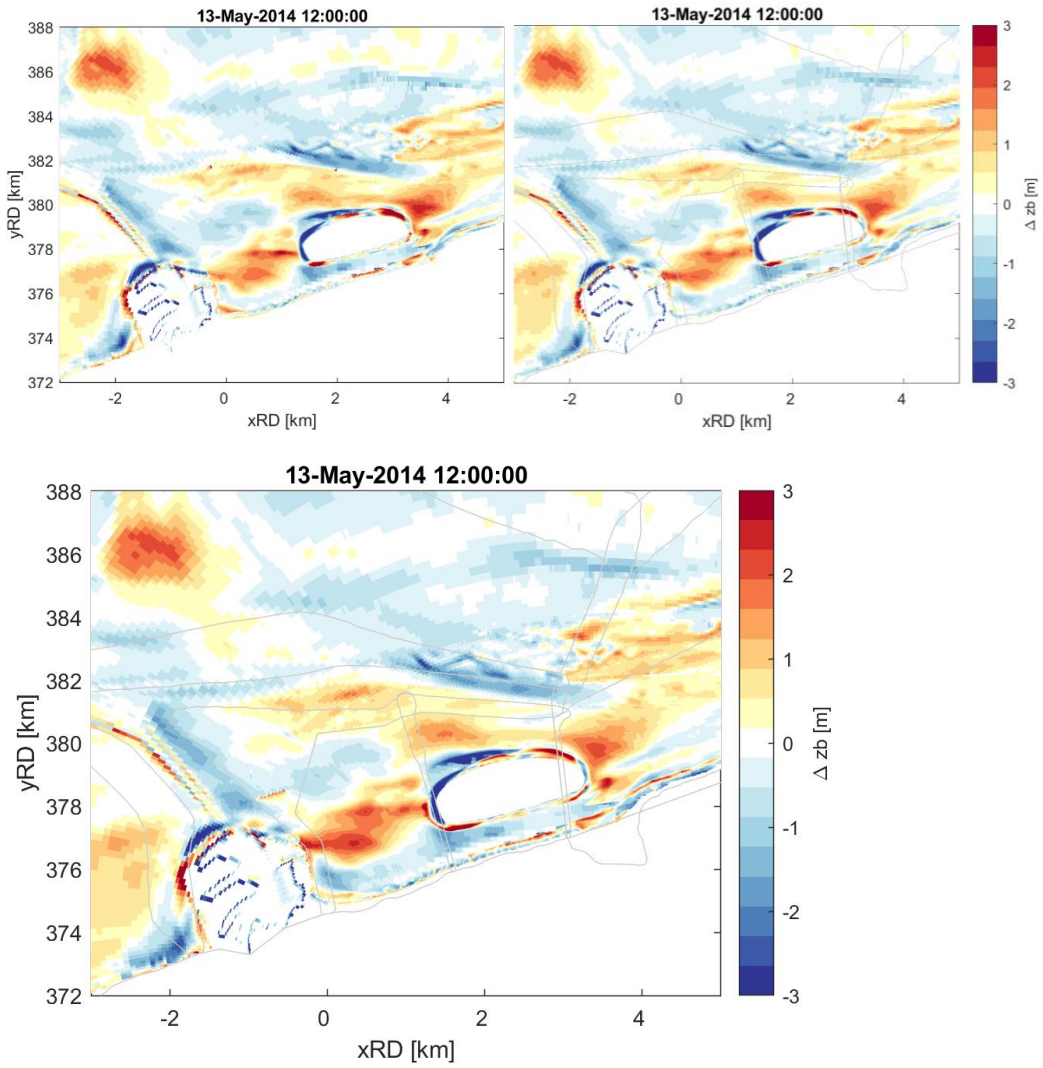

Figure 4.4 Comparison of the 10-year erosion-sedimentation pattern for D3D02 (upper left), FM02 (upper right) and FM04 (bottom). The domain-decompositioning boundaries for FM computations are plotted in thin light grey lines for reference and were identical in the two Delft3D-FM simulations.

4.2.3 Sediment transport

A pilot-island is expected to influence the longshore transport along the beaches of Knokke. The cumulative transport over eight transects drawn perpendicular to the Knokke beaches were computed and saved for all simulations. The transects extend from the landward domain boundary to approximately the 7-meter depth contour (Figure 4.5). From the reference simulations D3D01 and FM01 we can conclude that the transported masses of sediment match well between Delft3D-4 and Delft3D-FM (Figure 4.5). The total transport over the entire simulated period was eastwards for all transects. The cumulative transport increases from West to East in the reference simulations without a pilot island, e.g. D3D01, FM01 and FM02, leading to coastal erosion along these transects.

This behavior changes drastically with the pilot-island in place. The transport rates decrease strongly from x=10km eastwards, being the transects that lie sheltered by the pilot-island. This leads to a convergence zone around these transects, which is confirmed by the erosion/sedimentation pattern (Figure 4.4).
Differences up to 10% exist between Delft3D-4, Delft3D-FM without refinement and Delft3D-FM with refinement. On an identical grid, the FM total transports generally lie slightly below the Delft3D-4

transports. The grid refinement in combination with the pilot-island leads to an increase of computed longshore transports, but the transport with or without refinement in the reference simulations without pilot-island is almost the same. Therefore, these differences are attributed to a fine interplay between grid resolution and its effect on flow field and/or numerical scheme. Which of the model outcomes is most true can't be determined from a model-to-model comparison.

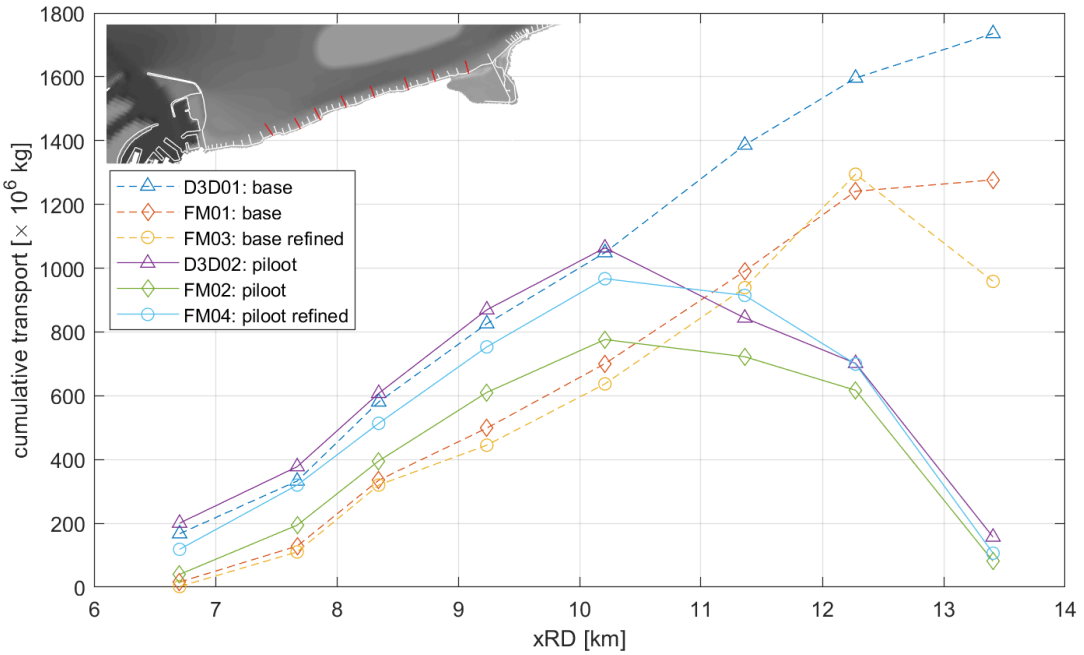

Figure 4.5 Cumulative suspended and bedload sediment transport along the nearshore of Knokke beaches plotted as a function of longshore x-coordinate. Transports were computed on the transects that are drawn on the inset bathymetry in red. Positive transport is towards the East.

4.2.4 Bed level change at the Paardenmarkt

Four transects are plotted in Figure 4.6 to assess the evolution of the pilot-island in the simulations D3D02, FM02 and FM04. The final transects between the three simulations are very similar but vary in the amount of erosion on the northwest side of the pilot-island (transect 1, Figure 4.6). The Delft3D-FM simulations erode to a gentler slope than the Delft3D-4 simulation does. With the local grid-refinement Delft3D-FM can maintain a steeper slope again.

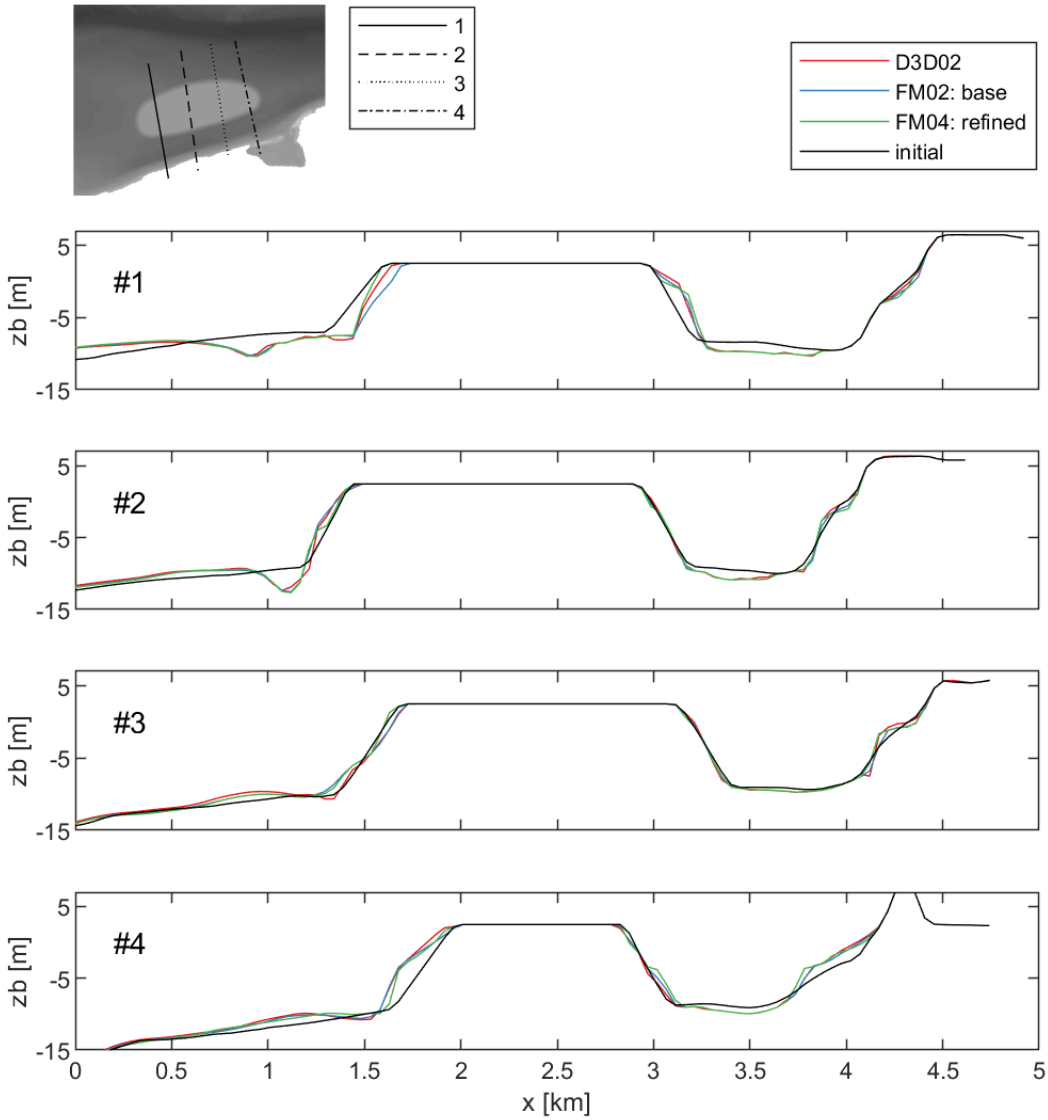

Figure 4.6 Comparison of evolution of 4 transects drawn along the Knokke beach in the reference simulations without pilot-island. The initial bathymetry in black for reference, blue the Delft3D-FM computation (FM01) and in red Delft3D-4 (D3D01).

Both Delft3D-4 and Delft3D-FM show the formation of a gully on the seaward side of the pilot-island in the two western profiles while the two eastern profiles show sedimentation on the foreshore. In these features there are no differences between the three simulations.

One possible cause for differences between the unrefined and the refined model outcomes is the grid-dependence of the implementation of eddy-viscosity and diffusion. The background values of viscosity and diffusion are kept constant in these model simulations but in reality, they depend on grid size. This could be circumvented by using a Smagorinsky type formulation for the viscosity instead of using constant background terms. This we did however not pursue further here because the effect on morphodynamics for this case appears limited.

4.2.5 Computational time

A local grid refinement affects the computational time in two ways. First, the number of grid cells gets increased. Because the chosen local refinement was placed in the area of the base grid with the finest resolution, this local refinement increased the number of cells from 101 to 191 thousand which is nearly a doubling. Secondly, the minimal cell area was reduced from 993 m^2 to 103 m^2.

This reduction is larger than a factor of 4 because the local refinement is connected to the base grid with triangles which typically have a cell area half the area of an adjacent quadrilateral.

Consequently, the computational time of the Delft3D-FM computation moved from 50.2 hour to 116.5 hour, see Table 4.2. This increase is mostly attributed to a reduction in average time-step (Figure 4.3) due to the Courant criterium. Regardless of the amount of 'small' grid cells in the domain, the timestep is determined by just one limiting cell and is then used for the whole domain. Although increase of number of cells is local, the timestep consequence of this refinement is not.

Next to that, the manual partitioning (Figure 3.12) that is imposed does not distribute the grid cells equally over the processors anymore. This is the most important reason why automatic partitioning of the domain is desirable. It is however considered only of secondary importance after the reduction of the average timestep.

Given the relatively small effect the local grid refinement had on the results we can conclude that the refinement was not strictly necessary after all. Given the doubling of the computational time, the original grid can suffice for scenario runs on this scale and time frame. Chapter 5.1 will expand on reasons and possible alternative approaches to local grid refinement.

Table 4.2 Computational times of discussed simulations

	Description	Partitions	Cluster	SUM	FLOW	WAVE
D3D01	D3D on base grid	1x4	Normal-e3	95	67	28
D3D02	D3D on base grid with pilot-island	1x4	Normal-e3	92	64	28
FM01	FM on base grid	2x4	Normal-e3	50	13	37
FM02	FM on refined grid	2x4	Normal-e3	61*	23*	38
FM03	FM on base grid with pilot-island	2x4	Normal-e3	126	89	37
FM04	FM on refined grid with pilot island	2x4	Normal-e3	117	77	40

** FM02 was run with a maximal timestep of 15 seconds instead of 30 to keep the simulation stable, which makes the comparison to FM01 unfair.*

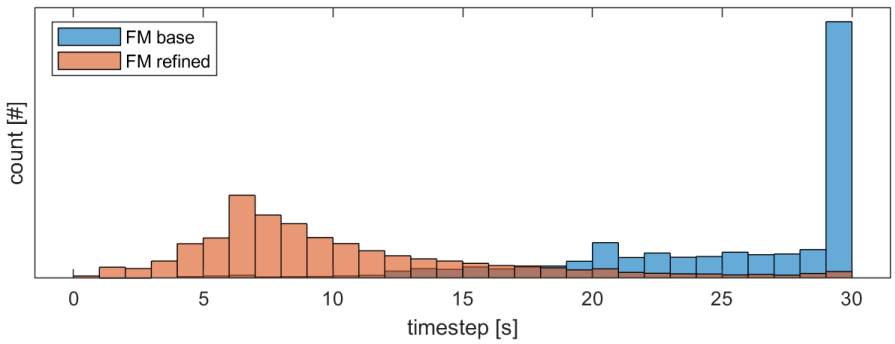

Table 4.3 Histograms of computational timestep of FM01 (blue) and FM04 (red)

5 Synthesis

5.1 Discussion

5.1.1 Delft3D-4 vs Delft3D-FM

Certain model approaches which were available in Delft3D-4 are not (yet) functioning in Delft3D-FM. These include Riemann boundary conditions as absorbing-generating offshore boundaries and with that the reflection coefficient alpha. Without these approaches, the model-data comparison still showed good results and the conversion to Delft3D-FM was not hindered by the absence of these functionalities. They do however prevent a fully automated conversion from the old model-suite to the new one.

Some functionality in Delft3D-FM is still under development. Carefree distribution of the workload of a simulation over multiple machines is still hindered by two aspects. In the discussed simulations, the scalability of computational times through parallel computing remained limited to two machines. This was because the WAVE computation was computed on a single domain and could not be partitioned. When parallelization of the wave computation becomes available, further reduction of computational time is anticipated. Next to that one has to be careful with domain partitioning around dredge and dump sites. One must manually ensure that no dredge or dump sites are crossed by the automatically generated domain decompositioning. If they do cross, these must be manually decomposed. This is again anticipated to be solved in future releases of Delft3D-FM.

5.1.2 Grid refinement

Because of the orthogonality criteria of a Delft3D-FM grid, the truly curvilinear grid of the VlaBa-model is not an ideal base grid for local refinements. A good base grid has cells with aspect-ratio close to 1:1, because the orthogonality criterium gets violated more strongly for connecting cells between base grid and local refinement for base grid cells with a large aspect-ratio. The landward boundary of the VlaBa base grid west of Zeebrugge Harbour has strongly skewed cells, so the grid refinement should ideally stay away from there.

The simulation results with and without grid refinement around the pilot-island did not show large discrepancies. Considering the doubling of computation time, the grid refinement was a good exercise but was not necessary to draw conclusions on the pilot-island's effect on the coastline on this timescale.

5.2 Conclusions

The comparison of hydrodynamics as computed by Delft3D-4 and Delft3D-FM improves confidence in the capabilities of morphodynamic modelling with Delft3D-FM. Hydrodynamics were validated against measurements of water level, depth-averaged flow velocity and wave height. This validation showed that Delft3D-FM performs equally well as Delft3D-4. Morphodynamics could only be compared model-to-model in absence of measurements. Minor differences in morphodynamic outcomes exist. These are assumed to be attributed to differences in numerical scheme, which accumulate in cumulative model output such as erosion/sedimentation or dredged volumes.

The computation time with Delft3D-FM is reduced by a factor 2 compared to Delft3D-4, mostly due to a flexible timestep that Delft3D-4 did not have. Further developments in domain decompositioning with Delft3D-FM are anticipated to improve parallel computing and therefore reduce computational time even more.
This refinement exercise has shown us that a good Delft3D-4 grid is not necessary the most optimal Delft3D-FM grid. A good base grid for Delft3D-FM would have a cell aspect-ratio near 1:1 for all

cells that are not connecting cells and follows the orientation of the depth contours near the coastline (which the VlaBa grid does not have in the entire domain). Reducing the grid size with a local refinement of factor 2 strongly affects the computational time step. This led, in combination with the increase of grid cells due to the refinement, to a doubling of the computational time. For this particular scenario the local refinement was not strictly necessary given the coherence in model outcomes with and without refinement.

For mid-term morphological models on 30-km scale, this report demonstrates that the 2DH morphodynamic functionality of Delft3D-4 such as Morphological acceleration, multiple sediment fractions, dredging and dumping work well in Delft3D-FM. Riemann boundaries were not successfully applied in Delft3D-FM in this case study.

5.3 Recommendations

10 Years of hydrodynamic and morphodynamic development of the Vlaamse Baaien region was shown to be simulated equally well by Delft3D-FM as with Delft3D-4. Therefore, this study gives confidence in developing the next generation morphodynamic models in the new model suite. Future studies of the Vlaamse Baaien region with Delft3D-FM should ideally use a designed-for-purpose unstructured grid with cell aspect ratio close to 1:1 in the entire domain for optimal use of flexible-mesh functionality.

6 References

De Maerschalck, B. et al., 2017. Modellering Belgische Kustzone en Scheldemonding Modellering Belgische Kustzone en Scheldemonding, Deelrapport 2 Morfologische analyse scenario's Vlaamse Baaien. WL Rapporten, 15_068_2, Waterbouwkundig Laboratorium & Deltares, Antwerpen, The Netherlands.

Martyr-Koller, R.C. et al., 2017. Application of an unstructured 3D fi nite volume numerical model to flows and salinity dynamics in the San Francisco Bay-Delta. Estuarine, Coastal and Shelf Science, 192, pp.86–107. Available at: http://dx.doi.org/10.1016/j.ecss.2017.04.024.

Van Rijn, L.C., 1993. Principles of sediment transport in rivers, estuaries, and coastal seas, Aqua Publications, Blokzijl, The Netherlands.

Röbke, B., Gawehn, M. & Van der Werf, J., 2018. The morphodynamic Delft3D-Vlaamse Baaien model. Report 1210301-001-ZKS-0007, Deltares, The Netherlands.

Vroom, J. Van Maren, B. Van der Werf, J.J. Van Rooijen, A., 2016. Zand-slib modellering voor het mondingsgebied van het Schelde-estuarium. Report 1210301-002-ZKS-002, Deltares, The Netherlands

Vroom, J., De Vet, P.L.M. & Van der Werf, J.J., 2015. Validatie waterbeweging Delft3D-NeVla model Westerscheldemonding. Report 1210301-001-ZKS-0001, Deltares, The Netherlands.

Deltares is an independent institute for applied research in the field of water and subsurface. Throughout the world, we work on smart solutions for people, environment and society.

Deltares

www.deltares.nl